ACS Partner Journal

ENVIRONMENT & HEALTH

Editors' Choice

Open Access

This article is licensed under CC-BY-NC-ND 4.0

pubs.acs.org/EnvHealth

Article

Uptake and Intracellular Fate of Fluorophore Labeled Metal−Organic-Framework (MOF) Nanoparticles

Ziyao Liu, Andreas Zimpel, Ulrich Lächelt, Maria Pozzi, Marta Gallego Gonzalez, Indranath Chakraborty, Stefan Wuttke, Neus Feliu,* and Wolfgang J. Parak*

Cite This: *Environ. Health* 2023, 1, 270−277

Read Online

ACCESS | Metrics & More | Article Recommendations | Supporting Information

ABSTRACT: The uptake and the fate of Zr-based metal−organic-framework nanoparticles labeled with organic fluorophores in HeLa cells has been monitored with fluorescence detection and elemental analysis. The nanoparticles have been selected as a model system of carrier nanoparticles (here Zr-based metal−organic-framework nanoparticles) with integrated cargo molecules (here organic fluorophores), with aze that does not allow for efficient exocytosis, a material which only partly degrades under acidic conditions as present in endosomes/lysosomes, and with limited colloidal stability. Data show that, for Zr-based metal−organic-framework nanoparticles of 40 nm size as investigated here, the number of nanoparticles per cells decreases faster due to particle redistribution upon proliferation than due to nanoparticle exocytosis and that, thus, also for this system, exocytosis is not an efficient pathway for clearance of the nanoparticles from the cells.

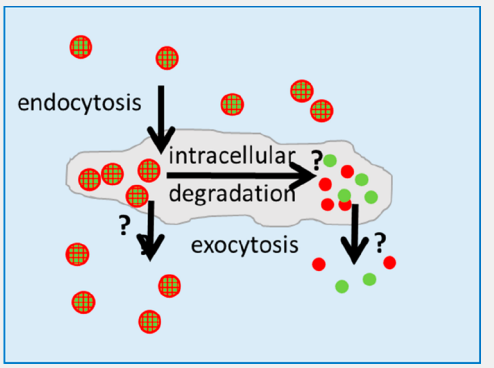

KEYWORDS: *nanoparticle endocytosis, exocytosis, proliferation, fate of nanoparticles, intracellular degradation, metal organic framework nanoparticles*

Downloaded via FRAUNHOFER-GESELLSCHAFT on February 20, 2024 at 10:48:37 (UTC).
See https://pubs.acs.org/sharingguidelines for options on how to legitimately share published articles.

INTRODUCTION

Upon exposure to cells, nanoparticles (NPs) are in general endocytosed,[1,2] whereby the kinetics is determined by their (bio)physicochemical properties. Inside cells, the NPs are located in vesicular compartments, i.e., endosomes/lysosomes. NPs are shared by daughter cells upon proliferation,[3,4] and NPs can also be excreted by cells via exocytosis.[5,6] While this is true for virtually all cells and NPs, the details obviously depend on the properties of the particular cells and NPs. Let us describe the entry and exit of NPs into/out of cells in terms of two parameters, the time-dependent number of NPs internalized per cell (i.e., intracellular NPs), and the time depend number of NPs remaining in the medium outside the cells (i.e., extracellular NPs). For this, we now consider three different basic processes. First, NPs in the vicinity of cells will be endocytosed, which increases the number of NPs per cell and lowers the number of NPs in the extracellular medium. Second, when NPs are exocytosed, the number of NPs per cell is reduced and the number of NPs in the extracellular medium increases. Third, when the NPs of one mother cell are shared between the two daughter cells, the number of NPs per cell is reduced but the number of NPs in the extracellular medium remains unaltered. All three processes are time-dependent, and different scenarios will happen with regard to how their kinetics compare. In cases in which endocytosis is slower than exocytosis and proliferation, cells will largely remain free of NPs, as endocytosed NPs would be immediately exocytosed or diluted by proliferation. Observations tell us that this is not the common case, as, in fact, NPs are found in most cells after exposure. Endocytosis works on a time scale of a few hours and, thus, is relatively fast. When endocytosis is the fastest of the three processes and exocytosis and proliferation could be neglected due to very long time scales, then the amount of NPs in cells would continuously increase. However, the common observation rather is that, after a certain time, the amount of internalized NPs per cell saturates. Frequently, it is suggested that this is because all NPs from the extracellular medium have already been ingested by the cells. However, measurements of the extracellular NP concentration show that there is a saturation of the intracellular NP concentration even if the reservoir of the extracellular NPs is infinite and the extracellular NP concentration is barely decreased upon endocytosis of NPs. This can only be explained by exocytosis and/or proliferation, and the outcome depends on whether exocytosis or proliferation is faster. When exocytosis is faster than proliferation, there will be a dynamic equilibrium of NPs entering cells via endocytosis and leaving them via exocytosis,

Received: June 10, 2023
Revised: August 12, 2023
Accepted: August 15, 2023
Published: September 3, 2023

ACS Publications

© 2023 The Authors. Co-published by Research Center for Eco-Environmental Sciences, Chinese Academy of Sciences, and American Chemical Society

https://doi.org/10.1021/envhealth.3c00075
Environ. Health 2023, 1, 270−277

while the mean number of NPs per cells would slightly raise due to endocytosis been faster than exocytosis.[7] When proliferation is faster than exocytosis, then NPs that have been internalized by cells will remain largely inside cells, though they are permanently redistributed between the different generations of daughter cells.[4,8] Whether exocytosis or proliferation dominates thus leads to very different outcomes. These outcomes, i.e., the time scales of exocytosis and proliferation, on the other hand would have impact on the clinical use of the NPs. Unfortunately, there are not many reports in the literature about quantitatively determined exocytosis rates of different NPs. Here there is still a demand for future studies. As the relation between proliferation rate and exocytosis rates depends on cells and NP properties, different scenarios can be expected.

Knowing the demands for the kinetics of NP entry and exit into and out of cells allows for designing the NPs up to this purpose. Cell proliferation depends on the type of cells and happens in general on a time scale of tens of hours. The detailed values can vary significantly between different cell types and can be determined easily by counting the cell number versus time.[9] We note that the proliferation rate largely depends on the conditions; i.e., diluted cell cultures will be different from confluent cell cultures and in particular from cells in tissue. Endo- and exocytosis depend on both the (bio)physicochemical properties of the NPs and the type of cells. There is a large set of data available in the literature about the dependence of endocytosis of NPs from NP size, state of agglomeration, surface charge, etc.[10] There is, however, scarce quantitative data available about the exocytosis of NPs.[5,11−13] Available data suggest that there is a strong size dependence, whereby smaller NPs can be exocytosed to a higher degree.[9] Tuning of the size of NPs thus allows for switching between exocytosis and proliferation as a dominant route for the reduction of the number of NPs per cell. Importantly, "size" is not a static but rather dynamic parameter. Upon degradation of the NPs, i.e., due to corrosion or enzymatic digestion, the NPs could be fragmented or even completely dissolved.[14−24] The intracellular fate of the NPs thus will also depend on their structural integrity over time.

For an experimental determination of endo- and exocytosis rates for different NPs (and their degradation fragments) and cells, it is highly recommended to measure also the number of NPs in the extracellular medium, i.e., the amount of extracellular NPs, in addition to the amount of intracellular NPs.[8] It is always a challenge to measure small deviations from big numbers. In the case of endocytosis, the (in general, initially large) amount of extracellular NPs may be reduced notably, but the amount of intracellular NPs will increase at any rate significantly. This is the opposite for exocytosis. After removal of noninternalized NPs, upon exocytosis (but not due to proliferation), there will be a significant increase in the amount of extracellular NPs, whereas only a fraction of the amount of intracellular NPs is lost due to exocytosis (or proliferation). Detection of the extracellular NP concentration thus allows for distinguishing between the effects of proliferation and exocytosis.

According to these lines the uptake and fate of gold NPs,[9] quantum dots with fluorophore labeled shell and preadsorbed proteins[7] and rare earth NPs[8] have been investigated. In these previous model systems, the NPs have a good size distribution and were also colloidally stable. In reality, these criteria of model systems may not always be fulfilled. For this reason, we applied the same methodology/principles to another NP system with less defined properties, where in particular colloidal stability is not sufficient to prevent agglomeration. According to this, as a model system, metal organic framework (MOF) NPs modified with organic fluorophores were chosen. Having cargo molecules (here organic fluorophores) loaded in a carrier NP (here MOF NPs) allows us also to probe for potential intracellular separation of the cargo molecules from the carrier NPs.

MOFs, which can also be made in particulate form, e.g., also as NPs, are an interesting material for delivery application.[25−29] Due to their highly defined porous nature, they can be loaded in a very controlled way with molecules, such as potential drugs. There are many studies about using MOFs in this way for intracellular delivery of drugs, and therefore it has relevance to know about the fate of these MOF NPs after they have been endocytosed by cells. Hereby, there are several questions of interest: (i) Will the MOF matrix degrade, which would automatically allow for a release of the drugs from the MOFs? (ii) If the MOF matrix does not degrade, will there still be intracellular desorption of the drug from the MOFs? (iii) Will the MOFs remain intracellular, or is there an efficient way of clearance from cells? While such questions are not easy to address in full detail, there are some key experiments that can be carried out in a straightforward way. When there is clearance of (parts of) MOFs from cells, in fresh medium around cells with internalized MOFs after some time there should be (parts of) MOFs to be found, which have been released by cells via exocytosis. When, upon exocytosis, parts of the molecules originally loaded into the MOF matrix are in the extracellular medium and no parts are on the MOF matrix (or vice versa), then one can conclude that, after cellular internalization, the loaded molecules must have come off the MOF matrix, as only in this way can both parts be exocytosed differently. In other words, a lot can be learned by analyzing what is found in the extracellular medium upon exocytosis. In this line in our study, we used MOFs loaded with fluorophores as model cargo molecules and studied their fate upon exposure to cells. The main interest here was to observe potential degradation of the MOF NPs and exocytosis of the respective fragments to investigate whether the fluorophores remain attached to the MOF NPs or are intracellularly detached.

MATERIALS AND METHODS

Zirconium-based metal−organic-framework NPs (Zr-MOF NPs) were prepared according to standard procedures.[30] The Zr-MOF NPs were fluorescence labeled by functionalization with an oligohistidine-ATTO647N conjugate (H6-A647N), in which the fluorophore (ATTO647N) is attached to an oligohistidine-tag (His-tags), as described previously by Röder et al.[31] The His-tag thereby bound to the Zr-MOF NPs by coordinative interaction.[31] Details of the H_6-A647N conjugate synthesis can be found in the Supporting Information. The physicochemical properties of the Zr-MOF NPs were characterized according to standard procedures,[8,32] including transmission electron microscopy (TEM), dynamic light scattering (DLS), zeta potential measurements, and elemental analysis upon degradation by inductively coupled plasma mass spectrometry (ICP-MS). For the uptake and fate studies, HeLa cells were exposed to the Zr-MOF NPs in serum-containing medium. For the uptake studies the amount of internalized Zr-MOF NPs was quantified after different exposure times t_{exp} and exposure concentrations $C_{Zr(add)}$ in terms of the mass concentration of elemental Zr. For the fate studies, after NP exposure for the time t_{exp} the remaining NPs in the extracellular medium were removed, and cells were incubated again for the time t_{inc}, after which the amount of internalized Zr-MOF NPs was

https://doi.org/10.1021/envhealth.3c00075
Environ. Health 2023, 1, 270−277

quantified. Quantification of the internalized Zr-MOFs was done by recording their fluorescence via flow cytometry or by measuring the intracellular (and extracellular) amount in terms of the elemental Zr concentration by ICP-MS.[8] Details for all experimental procedures are provided in the Supporting Information.

RESULTS AND DISCUSSION

Zr-MOF NP Synthesis and Characterization

The obtained Zr-MOF NPs had a relatively broad size distribution as measured by TEM (see Figure 1) with a mean

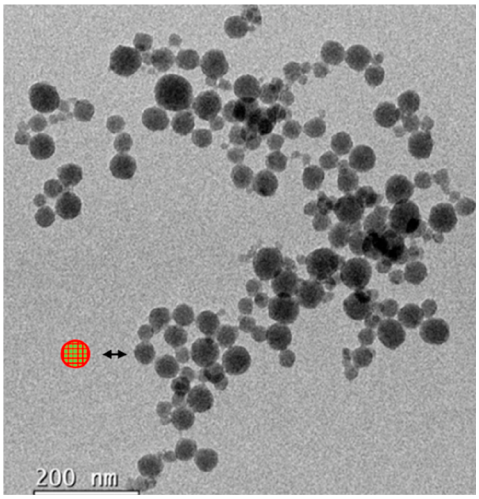

Figure 1. TEM image of the Zr-MOF NPs. Each of the dark spheres corresponds to one Zr-MOF NP. One Zr-MOF-NP as shown in the sketch provides contrast to TEM due to its inorganic matrix (depicted in red), in particular the Zr. The fluorophore label (as depicted in green) does not provide a contrast to TEM. The corresponding size distribution is shown in Figure S1.

NP diameter of d_c = 39 ± 11 nm (error is the standard deviation) (see Figure S1). There was no additional surface coating involved to increase colloidal stability such as done in other studies,[33] This resulted in partial agglomeration of the Zr-MOF NPs even in water, as indicated by the hydrodynamic diameter $d_{h(N)}$ = 117 ± 6 nm (error is the error of the mean) as obtained from the DLS number distribution (see Figure S2 and Table S1), which is significantly higher that the geometric NP diameter d_c. The Zr-MOF NPs had a slightly negative zeta-potential of $\zeta \approx -15$ mV (cf. Table S1), which is not enough to provide sufficient electrostatic repulsion to provide good colloidal stability. A metric for the concentration of the Zr-MOF NPs is provided in Figure S3.

In order to further probe the colloidal stability of the Zn-MOF NPs, their hydrodynamic diameter $d_{h(N)}$ was monitored over time by DLS upon exposure to buffers with different pH at different temperatures. There are two potential effects. Upon degradation of the Zr-MOF matrix, the NPs would decompose, i.e., leading to a smaller NP diameter. Upon further agglomeration, the NPs diameter would increase. Due to the already relatively broad initial size distribution of the Zr-MOF NPs, the DLS data only provide some trends, but no quantitative analysis is possible. As shown in Figure S4, the hydrodynamic diameter of the Zr-MOF NPs in Milli-Q water (pH ≈ 6.3) remains largely unchanged over time, even when temperature is elevated from room temperature (RT) to 37 °C. In the case of exposure to pH = 5, on the time scale of hours, degradation of the NPs can be observed (faster at 37 °C than at RT); i.e., there is some decrease in size, which levels off (i.e., there is no complete dissolution). Upon exposure to more acidic pH = 3.5, on the time scale of hours, there is an increase in size, which can be only explained by rising agglomeration. A likely scenario is that, at this low pH, there is also NP degradation, but large agglomeration results in increased NP sizes. Upon long-term exposure over days, in particular, for acidic conditions (pH = 3.5 and pH = 5) and elevated temperatures (T = 37 °C), there is massive agglomeration (see Figure S4). Addition of serum proteins (either bovine serum albumin (BSA) or fetal bovine serum (FBS)) or digestive enzymes (trypsin) did not lead to significant size changes over the time course of 2 days (Figure S5). Due to the larger error bars, however, no quantitative analysis was possible.

For this reason, alternative methods were used. With TEM (Figure S6 and Figure S7) it can be shown that, at pH = 6.3, (RT) the Zr-MOF NPs retain their shape over several weeks. However, under acidic conditions (pH = 3.5) already after 1 h it is no longer possible to identify individual Zr-MOF NPs, but instead, large heterogeneous agglomerates are present. X-ray diffraction analysis (XRD) showed that, even at neutral pH = 7.3, the Zr-MOF NPs lose crystallinity over time (Figure S8). At highly acidic pH = 3.5, XRD was not feasible due to degradation of the NPs. Degradation of the Zr-MOF NPs was also monitored by elemental analysis, in which Zr was detected over time in the supernatant above the NPs with ICP-MS. Data from Figure S9 show that, on the time course of hours, some Zr can be found in the supernatant above pelleted Zr-MOF NPs; i.e., some Zr has been released form the Zr-MOF NPs upon degradation. This effect is stronger for highly acidic pH = 3.5. However, there is no complete NP dissolution, but after some weeks, only a maximum 10% of the Zr was released from the NPs.

While all of these characterization data are affected by large error bars, in particular due to the initially broad size distribution and the low colloidal stability of the Zr-MOF NPs, the summary of the data give a conclusive qualitative picture, which is very similar to findings of similar materials.[8] A likely scenario is that, in solution, there is partial degradation and decomposition of the Zr-MOFs, which is triggered by low pH and elevated temperatures. The released degradation products, however, bind largely again to the NPs. In this way, most of the Zr remains in the NP phase and at maximum 10% is present as free ions. However, due to the dynamic equilibrium of degradation and rebinding, the structure of the MOF NPs is lost over time, in particular their crystallinity, resulting in large ill-defined agglomerates. As a result, none of the later described biological results can be related to precise physicochemical characteristics of the MOF-NPs, as those are unstable over time under conditions that resemble uptake via endocytosis by cells.

Exposure of HeLa Cells to Zr-MOF NPs

HeLa cells were exposed to Zr-MOF NPs in serum supplemented medium and incubated at 37 °C. The cell viability is shown in Figure S10. The elemental mass concentration $C_{Zr(add)}$ of Zr was used as a metric for the NP dose, as determined via ICP-MS (see Figure S3). Alternatively, the mass of Zr added per cell was used, which was calculated as $m_{Zr/cell(add)} = C_{Zr(add)} \cdot V_{well}/N_{cells/well}$, with $N_{cells/well}$ being the number of seeded cells per well and V_{well} being the volume of the culture medium containing the NPs in each well. As expected, the Zr-MOF NPs were endocytosed by the HeLa

https://doi.org/10.1021/envhealth.3c00075
Environ. Health 2023, 1, 270−277

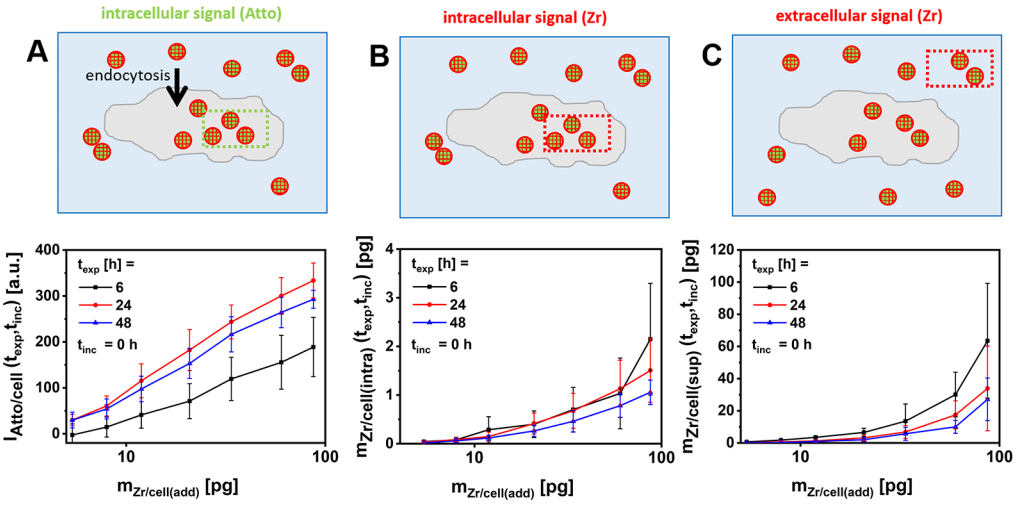

Figure 2. Cells are exposed to Zr-MOF NPs, leading to endocytosis of a fraction of the NPs at different concentrations $m_{Zr/cell(add)}$, i.e., the amount of Zr that has been added per seeded cell. The amount of NPs found in each cell was quantified in terms of A) intracellular fluorescence ($I_{Atto/cell}$) and B) intracellular Zr ($m_{Zr/cell(intra)}$). Also the amount of NPs remaining in the supernatant above the cells was quantified by C) the mass of extracellular Zr normalized to the number of cells present at the time of detection ($m_{Zr/cell(sup)}$).

cells, and thus, they are located in acidic intracellular vesicles, i.e., endosomes/lysosomes. TEM images show that the shape of internalized Zr-MOF NPs gradually becomes more ill-defined over time (Figure S11), as there is enhanced agglomeration. This is compatible with the degradation of the Zr-MOF NPs in acidic conditions (Figures S6 and S7), though inside the cells, the degree of degradation never reached the one demonstrated in the acidic test environments. Over the range of used NP exposure concentrations, no reduction in cell viability was observed (Figure S10). However, exposure to Zr-MOF NPs (leading also to their uptake, see Figure S12) moderately slowed the proliferation of the HeLa cells (Figure S13). It has been demonstrated in the past that cell proliferation is a more sensitive parameter than cell viability for monitoring the onset of NP induced impairment of cells.[34]

Uptake Study of Zr-MOF NPs by HeLa Cells

Zr-MOF NP uptake by cells was monitored with two independent methods. First, the amount of intracellular Zr-MOF NPs was quantified based on their Atto-647 fluorescence label with flow cytometry. Second, the amount of intracellular Zr-MOF NPs was quantified based on the amount of elemental Zr found in cells, as determined by ICP-MS (see Figure 2). With both techniques, a dose-dependent uptake behavior was determined; i.e., the more NPs are added per cell ($m_{Zr/cell(add)}$), the more intracellular fluorescence ($I_{Atto/cell}$) and intracellular Zr ($m_{Zr/cell(intra)}$) is detected. There is also a time dependence. In the case of flow cytometry, there is an increase in the amount of internalized NPs per cell within the first hours, but after 1 day there is a saturation and even a slight reduction (Figure 2A, Figure S12A). Note that flow cytometry records the fluorescence signal of single cells; i.e., when proliferation increased the cell number (Figure S13), there are more cells, and thus the fluorescence signal distributes to the daughter cells (Figure S14). If there would be no proliferation (i.e., the number of cells remained constant), then the fluorescence per cell would still increase further after 1 day of incubation of cells with the NPs, as there is continuous uptake of NPs. However, when there is continuous uptake of NPs and there is also proliferation, i.e., splitting of the internalized NPs between the daughter cells, then the amount of internalized NPs saturates over time.[35]

The ICP-MS data yield qualitatively the same trend, although there are quantitative differences. ICP-MS is an ensemble measurement. In the present example, the total mass of Zr in all cells is determined (Figure S15A). Likewise, the total mass of Zr remaining in the supernatant (i.e., the cell medium with added NPs) is determined (Figure S15B; the corresponding data describing the fate of the NPs after endocytosis are shown in Figure S16). As the number of cells increases over time (Figure S13), for obtaining the mass of intracellular/extracellular Zr per cell, the total mass of detected Zr has to be normalized by the number of cells present at the time of measurement (Figure 2B,C, Figure S17). The data show here that the mass of Zr per cell already saturates after 6 h of exposure (Figure 2B) and then slightly decays. Both flow cytometry data and ICP-MS data (Figure 2A versus Figure 2B) show that there is a saturation of intracellular Zr-MOF NPs after some time as expected,[36] but the time points for saturation as obtained by the two different measurements differ. Strictly speaking, the detailed reasons for this difference are not known. However, it has to be considered that two different techniques are applied (fluorescence detection and mass spectrometry), which detect two different parts of the NPs (Atto-647 and Zr). There can be fluorescence quenching due to different pH values in the endosomes/lysosomes, which in the case of Atto-647 is not high and the effect would go in the different direction and could not explain the increased fluorescence versus the saturated Zr. The matrix of the cells around the NPs can act as an optical element (e.g., a lens), which could change the fluorescence read-out. Also if the Atto-647 label would be degraded from the MOF matrix, and due to its small size exocytose, the fluorescence signal and the mass spectrometry signal would deviate, but again, this would not explain the increased fluorescence versus the saturated Zr (NP degradation will be discussed in more detail in Figure 4). This clearly shows that uptake data need to be interpreted very critically, as the result can depend on the used label and the detection technique. In studies with several independent repeats (here n = 4), there are also significant error bars.

https://doi.org/10.1021/envhealth.3c00075
Environ. Health 2023, 1, 270−277

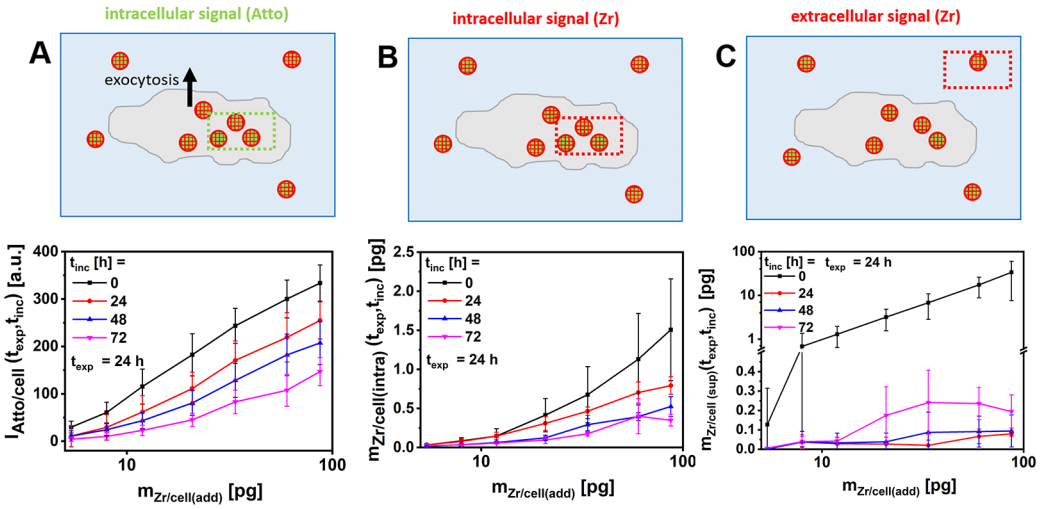

Figure 3. Cells were exposed to Zr-MOF NPs for the time t_{exp}, leading to endocytosis of a fraction of the NPs at different concentrations $m_{Zr/cell(add)}$. After this exposure, the cell medium containing noninternalized NPs was replaced by fresh cell medium. After further incubation for the time t_{inc}, the amount of NPs still found in each cell was quantified in terms of A) intracellular fluorescence ($I_{Atto/cell}$) and B) intracellular Zr ($m_{Zr/cell(intra)}$). Also the amount of NPs released to the medium by exocytosis was quantified by C) the mass of extracellular Zr normalized to the number of cells present at the time of detection ($m_{Zr/cell(sup)}$). Here t_{inc} = 0 refers to the measurement directly before exchange of the medium; i.e., here, still the NPs present in the exposure solution are present.

While there are thus quantitative differences, qualitatively a dose-dependent NP uptake can be confirmed, whereby the amount of intracellular NPs saturates over time.

The amount of Zr-MOF NPs that remain in the cell medium, i.e., the ones that are not endocytosed by cells, remains constant over time (Figure S15B). This is in agreement with previous studies that demonstrate that the NP-containing cell medium in general is an infinite reservoir of NPs, and while only a tiny fraction of NPs from the medium is endocytosed, the number of remaining NPs in the medium virtually does not change over time.[8,35] Thus, the reason why there is a saturation of the number of internalized NPs per cell over time is clearly not the fact that the extracellular medium is depleted of NPs but is due to the equilibrium of NP uptake by endocytosis and NP redistribution upon proliferation.[8,35] If the amount of NPs remaining in the cell medium is normalized to the number of cells over time (Figure 2C, Figure S17B), it can be seen that the amount of extracellular NPs per cell decreases over time. While the total amount of NPs in the medium remains virtually constant, the cell number increases over time, and thus the amount of extracellular NPs per cell decreased (Figure 2C). This means that, over time, more cells are competing for the uptake of the constant amount of NPs from the medium, which can explain the small decrease in NP uptake over time after the onset of saturation (Figure 2A,B).

Fate Study of Zr-MOF NPs in HeLa Cells

After the HeLa cells had been exposed for t_{exp} = 24 to Zr-MOF NPs, all residual NPs from the medium were washed away and cells were further incubated in fresh cell medium, without the addition of NPs. As after the washing no NPs are in the extracellular medium, NPs found after additional incubation time t_{inc} again in the extracellular medium must have gotten there by exocytosis (if one neglects the unlikely possibility of massive cell necrosis and lysis). In Figure 3, the loss of intracellular NPs and the small increase in extracellular NPs after washing are shown for different incubation times. The intracellular fluorescence due to the Atto-647 label of the Zr-MOF NPs as detected by flow cytometry decreases over time (Figure 3A, Figure S12B). This loss of intracellular fluorescence is largely due to proliferation. When the fluorescence signal is scaled by the ratio of the cell number during measurements versus the number of seeded cells, then there is no longer a decrease in fluorescence (Figure S14). In other words, the internalized NPs are continuously redistributed among the growing number of cells, and thus, the number of NPs per cell decreases. The same effect can be seen in the mass spectrometry measurements. The total amount of internalized NPs remained constant over time (Figure S16A). However, due to the increasing number of cells, the amount of NPs per cell goes down over time (Figure 3B, Figure S18A).

There is another uncertainty in comparing the flow cytometry and ICP-MS data from Figure 3. The Zr-MOF NPs could release either Zr ions or small MOF fragments upon intracellular degradation. ICP-MS cannot distinguish between Zr as free ions or Zr in small Zr-MOF NP fragments. But, due to the size dependence of exocytosis efficiency, the amount of exocytosed Zr will be different for ions and NP fragments as degradation products. For the Atto-647 fluorophore, the situation is even more complicated. While flow cytometry detection of intracellular Atto-647 does not depend on whether Atto-647 is free or attached to the Zr-MOF NPs, exocytosis of Atto-647 would be different. Upon intracellular degradation, Atto-647 could be released more easily from the Zr-MOF NPs, or it could still be bound to the released Zr-MOF NP fragments. The difference between both forms could not be detected with flow cytometry, but again, due to the size dependence of exocytosis, clearance of Atto-647 from the cells would be different for both cases.

After the Zr-MOF NPs supplemented medium was removed and replaced with new medium, almost no NPs could be detected in the supernatant above the cells (Figure S16B). The time point t_{inc} = 0 here shows the amount of NPs in the cell medium just before replacement of the medium, i.e., the concentration of extracellular NPs during the original exposure. After t_{inc} = 24 h, there are still almost no NPs in the extracellular medium. With ongoing time, more NPs are

https://doi.org/10.1021/envhealth.3c00075
Environ. Health 2023, 1, 270−277

exocytosed by cells and there are Zr-MOF NPs found in the medium, which is a very low amount in comparison to the original exposure concentration. Figure 3C and Figure S18B display the same data, albeit normalized to the cell count. These data again demonstrate that the massive loss in NPs per cells (Figure 3A,B) is due to proliferation. There is some exocytosis (Figure 3C), which reduces the number of NPs per cell less than the NP redistribution by proliferation. This is also in good agreement with a previous study with similar NPs.[8]

Concerning exocytosis, in our work measurements were done in terms of extracellular Zr detected by ICP-MS. In principle, inside ensomes/lysosomes, the Atto-647 label could have come off the Zr-MOF NPs and also could have been exocytosed independently, as known from other systems.[7] While we do not have data about exocytosed Atto-647, as due to the low concentrations, fluorescence determination of extracellular Atto-647 would be prone to large errors, we can compare the intracellular Atto-647 signal and the intracellular amount of Zr; see Figure 4 (and Figure S19). The Atto-647

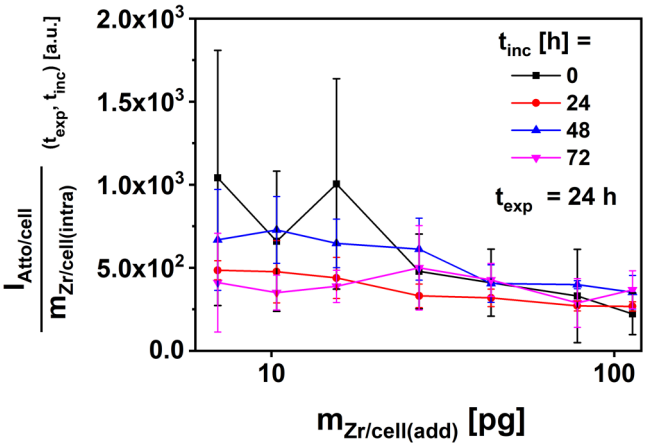

Figure 4. After the medium with extracellular Zr-MOF NPs had been substituted by fresh medium, the intracellular Atto-647 fluorescence (Figure 3A) and the intracellular Zr content (Figure 3B) were measured. Here the ratio of intracellular Atto-647 and intracellular Zr is shown.

signal is not quantitative in a sense that the fluorescence has not been calibrated to the number of intracellular Atto-647 molecules; i.e., from the fluorescence signal the absolute number of Atto-647 molecules per cell cannot be concluded. However, the fluorescence signal will be (with some limits in concentration) proportional to the number of intracellular Atto-647 molecules.

If Atto-647 was degraded from the Zr-MOF NPs and exocytosed faster than the Zr-MOF matrix, then the ratio of intracellular Atto-647 to intracellular Zr should decrease over time. Within the level of experimental error from our measurements, no conclusions can be drawn. While there is a time-dependent decrease of the Atto-647/Zr signal (Figure 4), this is observed only at the low exposure concentrations $m_{Zr/cell(add)}$. Here, the fluorescence signal is weak, and thus the experimental error is high, and thus the experimental error does not allow making a sound statement. In other words, our measurements do not allow verification of the falsified release of Atto-647 from the Zr-MOF NPs. With another, similar system it was reported that fluorophores can be stably embedded in MOFs, without significant intracellular leaching.[33]

CONCLUSIONS

In this study, HeLa cells were exposed to multicompartment NPs, comprising a fluorescence Atto-647 label and a Zr-containing MOF matrix. The colloidal properties of the Zr-MOF NPs were not very well-defined; in particular, their size distribution was relatively broad. In this way, this work shows what information about the uptake and fate of NPs by/in cells can be determined even for ill-defined NP samples. This makes it relevant for "practical" NP samples, such as NPs in several consumer products, as those typically also have, for example, large size distributions. In particular, for consumer products, the full life cycle of all constituents needs to be known to be able to make a sound risk assessment. A general observation is also that results depend on the detection technique, as, for example, in this work fluorescence and ICP-MS data only qualitatively agreed. Having several techniques to monitor and quantify the presence of NPs in cells helps to overstate results.

It has to be noted that, although Zr-MOF NPs were used in this study as NPs, there is nothing specific to Zr-containing NPs included in our study. The outcome of our study, in contrast, applies to a larger set of NP materials. The first criterion is size. The diameter of the Zr-MOF NPs is too large to allow for their efficient exocytosis. For other NP materials with similar sizes and above, one can expect the same general behavior: the NPs are shared by the daughter cells upon proliferation, but exocytosis is not an efficient pathway for NP clearance. Apart from the Zr-MOF NPs, this was also reported for Au NPs[9] and rare earth NPs,[8] The second important criterion will be intracellular degradability. Some materials may completely dissolve in the acidic environment of endosomes/lysosomes. Here the dissolution of the Zr-MOF NPs is weak, which was also the case for the similar studies with rare earth NPs,[8] and there should be even no dissolution for Au NPs.[9] Dissolution/fragmentation of the NPs could lead to sizes where exocytosis works efficiently, which would lead to NP clearance from cells. In this way, the results of this study should hold true in general for NPs with sizes above ca. 20−30 nm made from materials that do not effectively degrade/fragment in endosomes/lysosome.

In general, NPs are endocytosed in a size- and time-dependent manner. For the samples here, there is a maximum amount of NPs per cell, as cells proliferate, and thus internalized NPs are redistributed among the daughter cells. While under the used exposure conditions the medium is a virtually indefinite reservoir of NPs, as the number of cells increased upon proliferation, the amount of extracellular NPs per cells over time goes down. An average size of the NPs of around $d_c \approx 40$ nm diameter of the inorganic part as used in this study prevents efficient exocytosis, and thus, when NPs from the extracellular medium have been removed, ongoing reduction of the number of NPs per cell over time is largely due to proliferation and not due to exocytosis.

ASSOCIATED CONTENT

Supporting Information

The Supporting Information is available free of charge at https://pubs.acs.org/doi/10.1021/envhealth.3c00075.

Detailed description of the synthesis of zirconium-based metal−organic framework (Zr-MOFs) NPs; physico-

https://doi.org/10.1021/envhealth.3c00075
Environ. Health 2023, 1, 270−277

chemical characterizations of Zr-MOFs NPs; degradation studies of Zr-MOFs NPs using different systems; protocols and results for cell culture, cytotoxicity, and intracellular morphology changes of Zr-MOFs NPs; addition data of uptake and fate studies based on flow cytometry and ICP-MS and their comparison (PDF)

AUTHOR INFORMATION

Corresponding Authors

Neus Feliu − *Zentrum für Angewandte Nanotechnologie CAN, Fraunhofer-Institut für Angewandte Polymerforschung IAP, 20146 Hamburg, Germany;* orcid.org/0000-0002-7886-1711; Email: neus.feliu@physnet.uni-hamburg.de

Wolfgang J. Parak − *Center for Hybrid Nanostructures, Universität Hamburg, 22761 Hamburg, Germany;* orcid.org/0000-0003-1672-6650; Email: wolfgang.parak@uni-hamburg.de

Authors

Ziyao Liu − *Center for Hybrid Nanostructures, Universität Hamburg, 22761 Hamburg, Germany; Key Laboratory of Biological Nanotechnology of National Health Commission, Xiangya Hospital, Central South University, Changsha 410008, China*

Andreas Zimpel − *Department of Chemistry and Center for NanoScience (CeNS), LMU Munich, 81377 Munich, Germany*

Ulrich Lächelt − *Department of Pharmacy and Center for NanoScience (CeNS), LMU Munich, 81377 Munich, Germany; Department of Pharmaceutical Sciences, University of Vienna, 1090 Vienna, Austria;* orcid.org/0000-0002-4996-7592

Maria Pozzi − *Center for Hybrid Nanostructures, Universität Hamburg, 22761 Hamburg, Germany*

Marta Gallego Gonzalez − *Center for Cooperative Research in Biomaterials (CIC BiomaGUNE), Basque Research and Technology Alliance (BRTA), 20014 Donostia-San Sebastián, Spain*

Indranath Chakraborty − *Center for Hybrid Nanostructures, Universität Hamburg, 22761 Hamburg, Germany; School of Nano Science and Technology, Indian Institute of Technology Kharagpur, Kharagpur 721302, India;* orcid.org/0000-0003-4195-9384

Stefan Wuttke − *BCMaterials, Basque Center for Materials, Applications and Nanostructures, 48950 Leioa, Spain; IKERBASQUE, Basque Foundation for Science, 48009 Bilbao, Spain;* orcid.org/0000-0002-6344-5782

Complete contact information is available at: https://pubs.acs.org/10.1021/envhealth.3c00075

Notes

The authors declare no competing financial interest.

ACKNOWLEDGMENTS

This article was supported by the project HeatNMof (European Union's Horizon 2020 program). N.F. was funded by Fraunhofer Attract (Fraunhofer-Gesellschaft). Z.L. was supported by China Scholarship Council (CSC).

REFERENCES

(1) Canton, I.; Battaglia, G. Endocytosis at the nanoscale. *Chem. Soc. Rev.* **2012**, *41*, 2718−2739.

(2) Yameen, B.; Choi, W. I.; Vilos, C.; Swami, A.; Shi, J. J.; Farokhzad, O. C. Insight into nanoparticle cellular uptake and intracellular targeting. *J. Controlled Release* **2014**, *190*, 485−499.

(3) Summers, H. D.; Brown, M. R.; Holton, M. D.; Tonkin, J. A.; Hondow, N.; Brown, A. P.; Brydson, R.; Rees, P. Quantification of Nanoparticle Dose and Vesicular Inheritance in Proliferating Cells. *ACS Nano* **2013**, *7*, 6129−6137.

(4) Bourquin, J.; Septiadi, D.; Vanhecke, D.; Balog, S.; Steinmetz, L.; Spuch-Calvar, M.; Taladriz-Blanco, P.; Petri-Fink, A.; Rothen-Rutishauser, B. Reduction of Nanoparticle Load in Cells by Mitosis but Not Exocytosis. *ACS Nano* **2019**, *13*, 7759−7770.

(5) Bartczak, D.; Nitti, S.; Millar, T. M.; Kanaras, A. G. Exocytosis of peptide functionalized gold nanoparticles in endothelial cells. *Nanoscale* **2012**, *4*, 4470−4472.

(6) Chithrani, B. D.; Chan, W. C. W. Elucidating the mechanism of cellular uptake and removal of protein-coated gold nanoparticles of different sizes and shapes. *Nano Lett.* **2007**, *7*, 1542−1550.

(7) Carrillo-Carrion, C.; Bocanegra, A. I.; Arnaiz, B.; Feliu, N.; Zhu, D.; Parak, W. J. Triple-Labeling of Polymer-Coated Quantum Dots and Adsorbed Proteins for Tracing their Fate in Cell Cultures. *ACS Nano* **2019**, *13*, 4631−4639.

(8) Liu, Z.; Escudero, A.; Carrillo-Carrion, C.; Chakraborty, I.; Zhu, D.; Gallego, M.; Parak, W. J.; Feliu, N. Biodegradation of Bi-Labeled Polymer-Coated Rare-Earth Nanoparticles in Adherent Cell Cultures. *Chem. Mater.* **2020**, *32*, 245−254.

(9) Sun, X.; Gamal, M.; Nold, P.; Said, A.; Chakraborty, I.; Pelaz, B.; Schmied, F.; von Puckler, K.; Figiel, J.; Zhao, Y.; Brendel, C.; Hassan, M.; Parak, W. J.; Feliu, N. Tracking stem cells and macrophages with gold and iron oxide nanoparticles - The choice of the best suited particles. *Applied Materials Today* **2019**, *15*, 267−279.

(10) Iversen, T. G.; Skotland, T.; Sandvig, K. Endocytosis and intracellular transport of nanoparticles: Present knowledge and need for future studies. *Nano Today* **2011**, *6*, 176−185.

(11) Ho, L. W. C.; Yin, B.; Dai, G.; Choi, C. H. J. Effect of Surface Modification with Hydrocarbyl Groups on the Exocytosis of Nanoparticles. *Biochemistry* **2021**, *60*, 1019−1030.

(12) Oh, N.; Park, J. H. Surface chemistry of gold nanoparticles mediates their exocytosis in macrophages. *ACS Nano* **2014**, *8*, 6232−6241.

(13) Ho, L. W. C.; Chan, C. K. W.; Han, R.; Lau, Y. F. Y.; Li, H.; Ho, Y.-P.; Zhuang, X.; Choi, C. H. J. Mammalian Cells Exocytose Alkylated Gold Nanoparticles via Extracellular Vesicles. *ACS Nano* **2022**, *16*, 2032−2045.

(14) Schauer, A.; Redlich, C.; Scheibler, J.; Poehle, G.; Barthel, P.; Maennel, A.; Adams, V.; Weissgaerber, T.; Linke, A.; Quadbeck, P. Biocompatibility and Degradation Behavior of Molybdenum in an In Vivo Rat Model. *Materials* **2021**, *14*, 7776.

(15) Peuster, M.; Fink, C.; Wohlsein, P.; Bruegmann, M.; Gunther, A.; Kaese, V.; Niemeyer, M.; Haferkamp, H.; Schnakenburg, C. v Degradation of tungsten coils implanted into the subclavian artery of NewZealand white rabbits is not associated with local or systemic toxicity. *Biomaterials* **2003**, *24*, 393−399.

(16) Bindini, E.; Ramirez, M. d. l. A.; Rios, X.; Cossío, U.; Simó, C.; Gomez-Vallejo, V.; Soler-Illia, G.; Llop, J.; Moya, S. E. In Vivo Tracking of the Degradation of Mesoporous Silica through 89Zr Radio-Labeled Core-Shell Nanoparticles. *Small* **2021**, *17*, 2101519.

(17) Liu, J.; Wang, P.; Zhang, X.; Wang, L.; Wang, D.; Gu, Z.; Tang, J.; Guo, M.; Cao, M.; Zhou, H.; Liu, Y.; Chen, C. Rapid Degradation and High Renal Clearance of Cu3BiS3 Nanodots for Efficient Cancer Diagnosis and Photothermal Therapy in Vivo. *ACS Nano* **2016**, *10*, 4587−4598.

(18) Roy, S.; Liu, Z.; Sun, X.; Gharib, M.; Yan, H.; Huang, Y.; Megahed, S.; Schnabel, M.; Zhu, D.; Feliu, N.; Chakraborty, I.; Sanchez-Cano, C.; Alkilany, A. M.; Parak, W. J. Assembly and Degradation of Inorganic Nanoparticles in Biological Environments. *Bioconjugate Chem.* **2019**, *30*, 2751−2762.

(19) Ma, Z.; Bai, J.; Jiang, X. Monitoring of the Enzymatic Degradation of Protein Corona and Evaluating the Accompanying

Cytotoxicity of Nanoparticles. *ACS Appl. Mater. Interfaces* **2015**, *7*, 17614−17622.
(20) Espinosa, A.; Curcio, A.; Cabana, S.; Radtke, G.; Bugnet, M.; Kolosnjaj-Tabi, J.; Pechoux, C.; Alvarez-Lorenzo, C.; Botton, G. A.; Silva, A. K. A.; Abou-Hassan, A.; Wilhelm, C. Intracellular Biodegradation of Ag Nanoparticles, Storage in Ferritin, and Protection by a Au Shell for Enhanced Photothermal Therapy. *ACS Nano* **2018**, *12*, 6523−6535.
(21) Polikarpov, D. M.; Gabbasov, R. R.; Cherepanov, V. M.; Chuev, M. A.; Korshunov, V. A.; Nikitin, M. P.; Deyev, S. M.; Panchenko, V. Y. Biodegradation of Magnetic Nanoparticles in Rat Brain Studied by Mössbauer Spectroscopy. *IEEE Trans. Magn.* **2013**, *49*, 436−439.
(22) Mazuel, F.; Espinosa, A.; Luciani, N.; Reffay, M.; Le Borgne, R.; Motte, L.; Desboeufs, K.; Michel, A.; Pellegrino, T.; Lalatonne, Y.; Wilhelm, C. Massive Intracellular Biodegradation of Iron Oxide Nanoparticles Evidenced Magnetically at Single-Endosome and Tissue Levels. *ACS Nano* **2016**, *10*, 7627−7638.
(23) Soenen, S. J.; Parak, W. J.; Rejman, J.; Manshian, B. (Intra)Cellular Stability of Inorganic Nanoparticles: Effects on Cytotoxicity, Particle Functionality, and Biomedical Applications. *Chem. Rev.* **2015**, *115*, 2109−2135.
(24) Feliu, N.; Docter, D.; Heine, M.; Del Pino, P.; Ashraf, S.; Kolosnjaj-Tabi, J.; Macchiarini, P.; Nielsen, P.; Alloyeau, D.; Gazeau, F.; Stauber, R. H.; Parak, W. J. In vivo degeneration and the fate of inorganic nanoparticles. *Chem. Soc. Rev.* **2016**, *45*, 2440−2457.
(25) Horcajada, P.; Chalati, T.; Serre, C.; Gillet, B.; Sebrie, C.; Baati, T.; Eubank, J. F.; Heurtaux, D.; Clayette, P.; Kreuz, C.; Chang, J.-S.; Hwang, Y. K.; Marsaud, V.; Bories, P.-N.; Cynober, L.; Gil, S.; Férey, G.; Couvreur, P.; Gref, R. Porous metal-organic-framework nanoscale carriers as a potential platform for drug delivery and imaging. *Nat. Mater.* **2010**, *9*, 172−178.
(26) Linnane, E.; Haddad, S.; Melle, F.; Mei, Z.; Fairen-Jimenez, D. The uptake of metal-organic frameworks: a journey into the cell. *Chem. Soc. Rev.* **2022**, *51*, 6065−6086.
(27) Ringaci, A.; Yaremenko, A. V.; Shevchenko, K. G.; Zvereva, S. D.; Nikitin, M. P. Metal-organic frameworks for simultaneous gene and small molecule delivery in vitro and in vivo. *Chemical Engineering Journal* **2021**, *418*, 129386.
(28) Cai, M.; Chen, G.; Qin, L.; Qu, C.; Dong, X.; Ni, J.; Yin, X. Metal Organic Frameworks as Drug Targeting Delivery Vehicles in the Treatment of Cancer. *Pharmaceutics* **2020**, *12*, 232.
(29) Lawson, H. D.; Walton, S. P.; Chan, C. Metal-Organic Frameworks for Drug Delivery: A Design Perspective. *ACS Appl. Mater. Interfaces* **2021**, *13*, 7004−7020.
(30) Zahn, G.; Schulze, H. A.; Lippke, J.; König, S.; Sazama, U.; Fröba, M.; Behrens, P. A water-born Zr-based porous coordination polymer: Modulated synthesis of Zr-fumarate MOF. *Microporous Mesoporous Mater.* **2015**, *203*, 186−194.
(31) Röder, R.; Preiß, T.; Hirschle, P.; Steinborn, B.; Zimpel, A.; Höhn, M.; Rädler, J. O.; Bein, T.; Wagner, E.; Wuttke, S.; Lächelt, U. Multifunctional Nanoparticles by Coordinative Self-Assembly of His-Tagged Units with Metal-Organic Frameworks. *J. Am. Chem. Soc.* **2017**, *139*, 2359−2368.
(32) Huhn, J.; Carrillo-Carrion, C.; Soliman, M. G.; Pfeiffer, C.; Valdeperez, D.; Masood, A.; Chakraborty, I.; Zhu, L.; Gallego, M.; Yue, Z.; Carril, M.; Feliu, N.; Escudero, A.; Alkilany, A. M.; Pelaz, B.; del Pino, P.; Parak, W. J. Selected Standard Protocols for the Synthesis, Phase Transfer, and Characterization of Inorganic Colloidal Nanoparticles. *Chem. Mater.* **2017**, *29*, 399−461.
(33) Carrillo-Carrion, C.; Martinez, R.; Navarro Poupard, M. F.; Pelaz, B.; Polo, E.; Arenas-Vivo, A.; Olgiati, A.; Taboada, P.; Soliman, M. G.; Catalan, U.; Fernandez-Castillejo, S.; Sola, R.; Parak, W. J.; Horcajada, P.; Alvarez-Puebla, R. A.; del Pino, P. Aqueous Stable Gold Nanostar/ZIF-8 Nanocomposites for Light-Triggered Release of Active Cargo Inside Living Cells. *Angew. Chem.* **2019**, *58*, 7078−7082.
(34) Ma, X.; Hartmann, R.; Jimenez de Aberasturi, D.; Yang, F.; Soenen, S. J. H.; Manshian, B. B.; Franz, J.; Valdeperez, D.; Pelaz, B.; Feliu, N.; Hampp, N.; Riethmuller, C.; Vieker, H.; Frese, N.; Golzhauser, A.; Simonich, M.; Tanguay, R. L.; Liang, X.-J.; Parak, W. J. Colloidal Gold Nanoparticles Induce Changes in Cellular and Subcellular Morphology. *ACS Nano* **2017**, *11*, 7807−7820.
(35) Kang, Y.; Nack, L. M.; Liu, Y.; Qi, B.; Huang, Y.; Liu, Z.; Chakraborty, I.; Schulz, F.; Ahmed, A. A. A.; Clavo Poveda, M.; Hafizi, F.; Roy, S.; Mutas, M.; Holzapfel, M.; Sanchez-Cano, C.; Wegner, K. D.; Feliu, N.; Parak, W. J. Quantitative considerations about the size dependence of cellular entry and excretion of colloidal nanoparticles for different cell types. *ChemTexts* **2022**, *8*, 9.
(36) Ashraf, S.; Hassan Said, A.; Hartmann, R.; Assmann, M.-A.; Feliu, N.; Lenz, P.; Parak, W. J. Quantitative particle uptake by cells as analyzed by different methods. *Angew. Chem.* **2020**, *59*, 5438−5453.

Recommended by ACS

Intratumoral Biosynthesis of Gold Nanoclusters by Pancreatic Cancer to Overcome Delivery Barriers to Radiosensitization
Aaron S. Schwartz-Duval, Konstantin V. Sokolov, *et al.*
JANUARY 11, 2024
ACS NANO
READ

ROS-Responsive Fluorescent Sensor Array for Precise Diagnosis of Cancer via pH-Controlled Multicolor Gold Nanoclusters
Haifeng Lu, Qunlin Zhang, *et al.*
AUGUST 02, 2023
ACS APPLIED MATERIALS & INTERFACES
READ

High-Quantum-Yield Ultrasmall Ln_2O_3 (Ln = Eu, Tb, or Dy) Nanoparticle Colloids in Aqueous Media Obtained via Photosensitization
Tirusew Tegafaw, Gang Ho Lee, *et al.*
OCTOBER 19, 2023
LANGMUIR
READ

Association between Arsenic Methylation in Early Pregnancy and Gestational Diabetes Mellitus: A Prospective Cohort Study
Min Jiang, Qingqing Liu, *et al.*
OCTOBER 02, 2023
ENVIRONMENT & HEALTH
READ

https://doi.org/10.1021/envhealth.3c00075
Environ. Health 2023, 1, 270−277